

ANALYSIS OF THE STRESS–STRAIN STATE OF COMPLEX-SHAPED PLATES

A. Ya. Grigorenko, S. A. Pankrat'ev, and S. N. Yaremchenko

The problem of the stress–strain state of quadrangular complex-shaped plates is solved. The solutions of the boundary-value problem obtained with two numerical approaches are compared. One approach is based on discrete-continuous methods. In this approach, the system of governing equations is represented in new coordinates based on variations taking into account the plate geometry. Using spline-collocation, the two-dimensional boundary-value problem for the system of partial differential equations is reduced to one-dimensional one, which is solved by the numerical discrete-orthogonalization method. The other (discrete) approach is based on the finite-element method. The results for trapezoidal plates designed with both approaches are compared. The values of the displacements determined agree with high accuracy.

Keywords: stress–strain state, plates of different shapes, coordinate transformation, discrete-continuous method, finite-element method, comparison of results

Introduction. Methods and approaches for determining the stress–strain state (SSS) of plates have been developed for many decades. Currently, many problems for plates of relatively simple shape have been solved analytically or semianalytically, using, in particular, series expansion and spline-approximation [6, 16]. Many studies are devoted to numerical methods of analysis of parallelogram-shaped plates under various boundary and loading conditions [5, 8, 14, 15, 20].

Special numerical approaches usually either allow for symmetry or use parametrization to describe the original domain [12, 19]. The application of coordinate transformation was discussed in [13, 18].

An approach to determining the SSS of quadrangular plates in refined statement using the spline-collocation and discrete-orthogonalization methods is presented in [10]. This approach uses the transformation from an arbitrary quadrangular domain to a rectilinear one [4, 17]. In [9], a similar transformation is used to determine the natural frequencies of plates and membranes. The stress state of trapezoidal plates and parallelogram plates is analyzed in [12], parametrizing the domain by other methods.

It is obvious that this problem can easily be solved using commercial FEM software. In this case, however, the problem of reliability of the results arises. The application of the FEM in designing plates is outlined in [7].

The goal of the present paper is comparative analysis of the SSS of complex-shaped plates (including quadrangular plates with convex geometry) using an approach based on the sequential application of the spline-collocation method, discrete orthogonalization method, and FEM.

1. Starting Equations. Let us consider isotropic plates of constant thickness in refined statement in a Cartesian coordinate system x, y using Timoshenko's hypotheses [2].

The bending and torsion strains $\kappa_x, \kappa_y, \kappa_{xy}$ and the angles of the rectilinear element γ_x, γ_y can be represented in terms of the total angles ψ_x, ψ_y and deflection w :

$$\kappa_x = \frac{\partial \psi_x}{\partial x}, \quad \kappa_y = \frac{\partial \psi_y}{\partial y}, \quad 2\kappa_{xy} = \frac{\partial \psi_x}{\partial y} + \frac{\partial \psi_y}{\partial x}, \quad \gamma_x = \psi_x + \frac{\partial w}{\partial x}, \quad \gamma_y = \psi_y + \frac{\partial w}{\partial y}. \quad (1)$$

The elasticity relations for the moments M_x , M_y , M_{xy} and shearing forces Q_x and Q_y for an isotropic plate take the following form [2]:

$$\begin{aligned} M_x &= D(\kappa_x + \nu\kappa_y), & M_y &= D(\kappa_y + \nu\kappa_x), & M_{xy} &= \frac{Gh^3}{6} \kappa_{xy}, \\ Q_x &= \frac{5}{6} Gh\gamma_x, & Q_y &= \frac{5}{6} Gh\gamma_y, \end{aligned} \quad (2)$$

where $D = \frac{Eh^3}{12(1-\nu^2)}$, $G = \frac{E}{2(1+\nu)}$, ν is Poisson's ratio; E is the elastic modulus; h is the plate thickness.

The equilibrium equations of the plate acted upon by a load q distributed uniformly over the whole surface are

$$\frac{\partial Q_x}{\partial x} + \frac{\partial Q_y}{\partial y} + q = 0, \quad \frac{\partial M_x}{\partial x} + \frac{\partial M_{xy}}{\partial y} + Q_x = 0, \quad \frac{\partial M_y}{\partial y} + \frac{\partial M_{xy}}{\partial x} + Q_y = 0. \quad (3)$$

Substituting (1) into (2) and (2) into (3), we obtain governing equations for the angles and deflection:

$$\begin{aligned} \frac{\partial \psi_x}{\partial x} + \frac{\partial^2 w}{\partial x^2} + \frac{\partial \psi_y}{\partial y} + \frac{\partial^2 w}{\partial y^2} &= -\frac{6q}{5Gh}, \\ D \left(\frac{\partial^2 \psi_x}{\partial x^2} + \nu \frac{\partial^2 \psi_y}{\partial x \partial y} \right) + \frac{Gh}{6} \left(\frac{h^2}{2} \left[\frac{\partial^2 \psi_x}{\partial y^2} + \frac{\partial \psi_y}{\partial x \partial y} \right] - 5 \left[\psi_x + \frac{\partial w}{\partial x} \right] \right) &= 0, \\ D \left(\frac{\partial^2 \psi_y}{\partial y^2} + \nu \frac{\partial^2 \psi_x}{\partial x \partial y} \right) + \frac{Gh}{6} \left(\frac{h^2}{2} \left[\frac{\partial^2 \psi_y}{\partial x^2} + \frac{\partial \psi_x}{\partial x \partial y} \right] - 5 \left[\psi_y + \frac{\partial w}{\partial y} \right] \right) &= 0. \end{aligned} \quad (4)$$

Let the potential strain energy of the plate for solving the FEM problem be described by

$$\Pi = \frac{1}{2} \iint_S (M_x \kappa_x + M_y \kappa_y + 2M_{xy} \kappa_{xy} + Q_x \gamma_x + Q_y \gamma_y - 2qw) dx dy, \quad (5)$$

where S is the plate area.

Considering (1) and (2), we get

$$\begin{aligned} \Pi &= \frac{1}{2} \iint_S \left\{ D \left[\left(\frac{\partial \psi_x}{\partial x} \right)^2 + \left(\frac{\partial \psi_y}{\partial y} \right)^2 + 2\nu \frac{\partial \psi_x}{\partial x} \frac{\partial \psi_y}{\partial y} \right] + \frac{Gh^3}{12} \left(\frac{\partial \psi_x}{\partial y} + \frac{\partial \psi_y}{\partial x} \right)^2 \right. \\ &\quad \left. + \frac{5Gh}{6} \left[\left(\psi_x + \frac{\partial w}{\partial x} \right)^2 + \left(\psi_y + \frac{\partial w}{\partial y} \right)^2 \right] - 2qw \right\} dx dy. \end{aligned} \quad (6)$$

To determine the deflection and angles, formulas (4) and (6) should be supplemented by the boundary conditions on the plate edge.

2. Problem Solving Methods.

2.1. Coordinate Transformation. The spline-collocation method in combination with the discrete orthogonalization method can only be applied to rectangular domains. Therefore, to transform a quadrangular domain into a rectangular one, we will use new coordinates ξ, η , which are related to x, y as follows [4]:

$$x = a_1 + a_2 \xi + a_3 \eta + a_4 \xi \eta,$$

$$y = b_1 + b_2 \xi + b_3 \eta + b_4 \xi \eta. \quad (7)$$

The coefficients a_i and b_i are determined from a system of eight linear equations by substituting into (6) four points (x_i, y_i) in the previous system and four points (ξ_i, η_i) in the new one. If, for example, $(\xi_i, \eta_i) = (\pm 1, \pm 1)$, transformation (6) becomes

$$x = \sum_{i=1}^4 x_i N_i, \quad y = \sum_{i=1}^4 y_i N_i, \quad (8)$$

where N_i are the shape functions of the quadrangular finite element of the first order [1]:

$$N_i = (1 + \xi \xi_i)(1 + \eta \eta_i) / 4.$$

In what follows, we will express all the derivatives with respect to x, y in terms of the derivatives with respect to ξ, η . The transformation formulas for the first derivatives of an arbitrary function f are

$$\frac{\partial f}{\partial x} = \left(\frac{\partial f}{\partial \xi} \frac{\partial y}{\partial \eta} - \frac{\partial f}{\partial \eta} \frac{\partial y}{\partial \xi} \right) / J, \quad \frac{\partial f}{\partial y} = \left(\frac{\partial f}{\partial \eta} \frac{\partial x}{\partial \xi} - \frac{\partial f}{\partial \xi} \frac{\partial x}{\partial \eta} \right) / J, \quad (9)$$

where J is the Jacobian of transformation (7). With (9), we can get explicit expressions for the second derivatives.

2.2. Spline-Collocation Method. Let us map the original quadrangle onto the square $[0, 1] \times [0, 1]$, as in [10], and substitute into (4) the expressions for the derivatives with respect to x, y in terms of the derivatives with respect to ξ, η . As a result, we get the equation

$$L\bar{u} = 0, \quad (10)$$

where L is a linear differential operator of the second order within the domain ξ, η ; $\bar{u} = \{w, \psi_x, \psi_y\}$ is an unknown vector. The clamped boundary condition is $\bar{u} = \bar{0}$. If the boundary is free and parallel to the axis Oy , then the boundary conditions are $M_x = 0, Q_x = 0, M_{xy} = 0$.

According to the spline-collocation method, the solution of the boundary-value problem (10) can be represented as

$$w = \sum_{i=0}^N w_i(\xi) \varphi_{1i}(\eta), \quad \psi_x = \sum_{i=0}^N \psi_\xi(\xi) \varphi_{2i}(\eta), \quad \psi_y = \sum_{i=0}^N \psi_{y_i}(\xi) \varphi_{3i}(\eta), \quad (11)$$

where w_i, ψ_ξ , and ψ_{y_i} are unknown functions of the coordinate ξ ; φ_i are linear combinations of cubic B -splines satisfying the boundary conditions $\eta = \text{const}$ at the edges. Substituting (11) into (10) and the boundary conditions and requiring them to be satisfied at $N + 1$ collocation points, we arrive at an one-dimensional boundary-value problem to be solved with the discrete-orthogonalization method [1.11].

2.3. Finite-Element Method. To approximate the solution, we choose the same functions as for the approximation of coordinates (7). For simplicity, we will use the quadrangular finite elements

$$w = \sum_{i=1}^4 w_i N_i, \quad \psi_x = \sum_{i=1}^4 \psi_\xi N_i, \quad \psi_y = \sum_{i=1}^4 \psi_{y_i} N_i, \quad (12)$$

where w_i, ψ_ξ , and ψ_{y_i} are the deflection and total angles at nodal points.

Substituting (12) into (5) and employing the Ritz method, i.e., differentiating with respect to w_j, ψ_{xj} , and ψ_{yj} , we get a system of linear algebraic equations for the deflection and angles at the nodes for an element with area S_k :

$$\iint_{S_k} \left(\frac{5}{3} Gh(\psi_\xi N_i + w_i N_\xi) N_{xj} + \frac{5}{3} Gh(\psi_{y_i} N_i + w_i N_{y_i}) N_{yj} - 2q N_j \right) dx dy = 0,$$

$$\iint_{S_k} \left\{ D(\psi_\xi N_\xi) N_{xj} + Dv(\psi_{y_i} N_{y_i}) N_{xj} + \frac{Gh^3}{12} (\psi_\xi N_{y_i} + \psi_{y_i} N_\xi) N_{yj} + \frac{5}{6} Gh(\psi_\xi N_i + w_i N_\xi) N_j \right\} dx dy = 0,$$

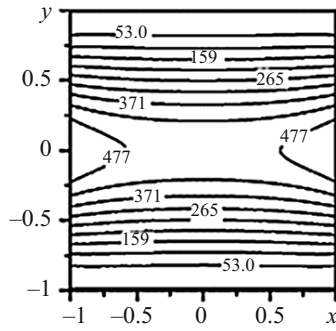


Fig. 1

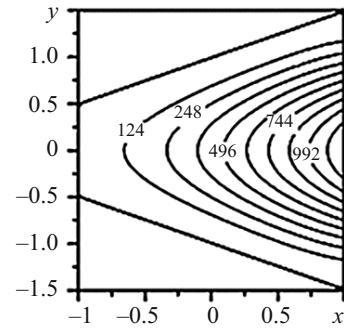


Fig. 2

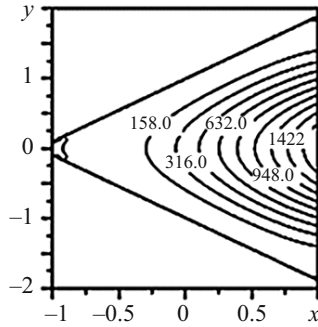


Fig. 3

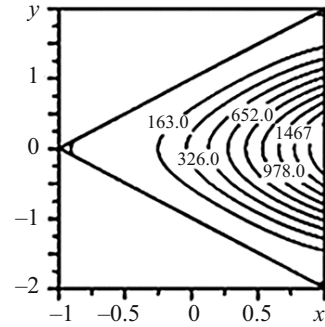


Fig. 4

$$\iint_{S_k} \left\{ D(\psi_{yi} N_{yi}) N_{yj} + Dv(\psi_{\xi} N_{\xi}) N_{yj} + \frac{Gh^3}{12} (\psi_{\xi} N_{yi} + \psi_{yi} N_{\xi}) N_{xj} + \frac{5}{6} Gh(\psi_{yi} N_i + w_i N_{yi}) N_j \right\} dx dy = 0, \quad (13)$$

where the summation is over double indices (the sign of summation over i is omitted); $N_{\xi} = \frac{\partial N_i}{\partial x}$ and $N_{yi} = \frac{\partial N_i}{\partial y}$ are determined

by (9). To evaluate the integrals in (13) with the Gaussian method, it is necessary to apply transformation (8) because $\iint_{S_k} f(x, y) dx dy = \int_{-1}^1 \int_{-1}^1 f(\xi, \eta) J d\xi d\eta$. Note that expressions (13) can also be derived by applying the Galerkin method to (5).

According to (5) and (13), the governing equations of the Ritz and Galerkin methods coincide. The governing system for the whole domain can be obtained by calculating and aggregate the coefficients of the systems for all the k elements.

3. Numerical Results. Using the above approaches, we have analyzed the SSS of plates whose outline and deflection distributions wE/q are shown in Figs. 1–4. One plate is square with side length equal to 2. The other two plates are isosceles trapeziums with such apexes that the quadrangle area remains constant. The bases of the trapezium are equal to 1 and 3 in Fig. 2 and to 0.2 and 3.8 in Fig. 3. The coordinates of the apexes are collected in Table 1.

The following parameter values were used: $h = 0.1, \nu = 0.3$. The trapezium bases are free, and the sides are clamped. The figures show the results obtained with the spline-collocation and discrete-orthogonalization methods using 60 collocation points and 1500 integration points.

In using the FEM, the square $[0, 1] \times [0, 1]$ was divided into elements with sizes $[0, 1/200] \times [0, 1/200]$. Formula (7) was then used to determine the coordinates of the nodes of the finite elements in the coordinates x, y . The resulting matrix is $3 \times 201 \times 201$, while the band width is 3×203 . Such an approach made it possible to obtain results (Table 2) in agreement with those obtained with the above two methods. To solve the systems of linear algebraic equations, the Gaussian method was used. Table 2 compares the maximum deflections wE/q achieved at the point $x = 1, y = 0$ in the first four plates. We failed to calculate the deflection of the trapezium close to a triangle (with bases 0.02 and 3.98). This problem was solved with the FEM, the maximum deflection ($wE/q = 1617.7$) differing from that for the trapezium (plate No. 3) insignificantly.

TABLE 1

Plate No.	Coordinates of the points defining the plate shape							
	x_1	y_1	x_2	y_2	x_3	y_3	x_4	y_4
1	-1	1	-1	-1	1	-1	1	1
2	-1	0.5	-1	-0.5	1	-1.5	1	1.5
3	-1	0.1	-1	-0.1	1	-1.9	1	1.9
4	0	1	-1	0	1	-2	1	2
5	0	1	4	0	4	4	0	4
6	0	1	4	0	4	4	0	5
7	0	1	4	0	4	4	0	3.5
8	0	1	4	0	4	4	0	4.25

TABLE 2

Plate No.	1	2	3	4
$w_{\max}E/q$, spl. coll./ DO	529.34	1235.6	1576.7	1628.5
$w_{\max}E/q$, FEM	527.75	1231.6	1570.8	1622.2

TABLE 3

Plate No.	Method	$w_{\max}E/q$	x	y
5	spl./DO	3161.5	1.5226	2.3299
	FEM	3144.1	1.52	2.3269
6	spl./DO	7790.9	0	2.8746
	FEM	7736.4	0	2.88
7	spl./DO	2315.6	1.9413	2.1480
	FEM	2303.3	1.94	2.1449
8	spl./DO	4016.4	0	2.5578
	FEM	3990.9	0	2.56

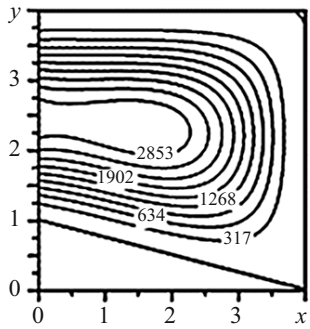


Fig. 5

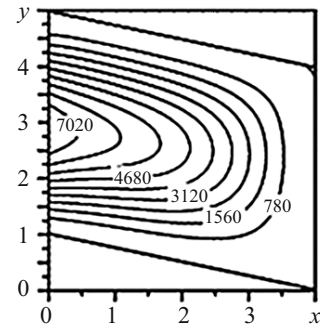


Fig. 6

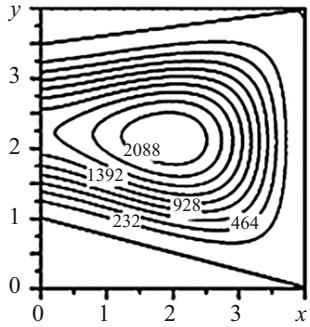


Fig. 7

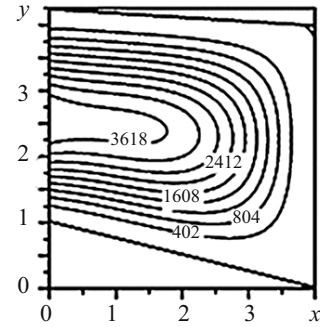


Fig. 8

The SSS of the triangle (plate No. 4) was determined with both approaches. To this end, three points of the four were placed on the same line for the quadrangle to degenerate into a triangle. If the first apex had coordinates $(-1; 0)$, the other apexes of the “quadrangle” (anticlockwise) were $(1; -2)$, $(1; 2)$ and, for example, $(0; 1)$. The reliability and accuracy of this calculation can be judged by comparing the maximums obtained for plate No. 3 and the trapezium with bases 0.02 and 3.98.

Also, we have determined the deflections of plates Nos. 5–8 (presented in Figs. 5–8), whose apex coordinates are in Table 1. The first three points are common to all the plates, while the fourth one shifts along the line $x = 0$. The side $x = 0$ is free, while the others are clamped. The deflection maximums and the corresponding points determined with the different methods are summarized in Table 3.

From Figs. 5–8 it follows that the shape of the deflection surface is strongly dependent on the shape and area of the plate. The maximum deflection for plate No. 6 with the largest area (Fig. 6) exceeds the deflection of plate No. 7 with the smallest area (Fig. 7) by more than three times. Tables 2 and 3 indicate that the relative difference between the results obtained with the two methods does not exceed 1%.

Conclusions. We have analyzed the stress–strain state of quadrangular plates of complex shape. The boundary-value problem has been solved using two numerical approaches, one of which is based on discrete-continuous methods and represents the governing system of equations in new coordinates based on changes that allow for the plate geometry. Using the spline-collocation, the two-dimensional boundary-value problem for the system of partial differential equations has been reduced to a one-dimensional problem, solved with the numerical discrete-orthogonalization method. The second (discrete) approach is based on the finite-element method. The results obtained for trapezoidal plates with both approaches have been compared. The displacements determined agree with high accuracy.

REFERENCES

1. S. K. Godunov, "Numerical solution of boundary-value problems for systems of linear ordinary differential equations," *Usp. Mat. Nauk*, **16**, No. 3, 171–174 (1961).
2. Ya. M. Grigorenko, A. T. Vasilenko, and G. P. Golub, *Statics of Anisotropic Shells with Finite Shear Stiffness* [in Russian], Naukova Dumka, Kyiv (1987).
3. O. C. Zienkiewicz, *The Finite-Element Method in Engineering Science*, McGraw-Hill, New York (1971).
4. M. S. Kornishin, V. N. Paimyshin, and V. F. Snegirev, *Computational Geometry in Problems of Shell Mechanics* [in Russian], Nauka, Moscow (1989).
5. R. S. Alwar and N. Ramachandra Rao, "Nonlinear analysis of orthotropic skew plates," *AIAA J.*, **11**, No. 4, 495–498 (1973).
6. V. Birman, *Plate Structures*, Springer, New York (2011).
7. J. Blaauwendraad, *Plates and FEM Surprises and Pitfalls*, Springer, New York (2010).
8. D. N. Buragohain and S. C. Patodi, "Large deflection analysis of skew plates by lumped triangular element formulation," *Comput. Struct.*, **9**, 183–189 (1978).
9. O. Civalek and M. Gurses, "Frequency analysis of trapezoidal plates and membrane using discrete singular convolution," *Asian J. Civil Eng. (Building and Housing)*, **9**, No. 6, 593–605 (2009).
10. A. Ya. Grigorenko, S. A. Pankrat'ev, and S. N. Yaremchenko, "Solution of stress–strain problems for complex-shaped plates in a refined formulation," *Int. Appl. Mech.*, **53**, No. 3, 326–333 (2017).
11. Ya. M. Grigorenko, A. Ya. Grigorenko, and G. G. Vlaikov, *Problems of Mechanics for Anisotropic Inhomogeneous Shells Based of Different Models*, Akademperiodika, Kyiv (2009).
12. N. N. Kryukov, "Design of oblique and trapezoidal plates with the use of spline functions," *Int. Appl. Mech.*, **33**, No. 5, 414–417 (1997).
13. W. Y. Li, Y. K. Cheung, F. Asce, and L.G. Tham, "Spline finite strip analysis of general plates," *J. Eng. Mech.*, **112**, 43–54 (1986).
14. P. Malekzadeh and A. R. Fiouz, "Large deformation analysis of orthotropic skew plates with nonlinear rotationally restrained edges using DQM," *Compos. Struct.*, **80**, No. 2, 196–206 (2007).
15. P. Malekzadeh and G. Karami, "Differential quadrature nonlinear analysis of skew composite plates based on FSDT," *Eng. Struct.*, **28**, 1307–1318 (2006).
16. P. Mohajerani, "The thick orthotropic plates analysis method, Part 1: A review," *IOSR J. Mech. Civil Eng.*, **12**, No. 2, Ver. III, 69–77 (2015).
17. V. N. Paimushin and S. V. Andreev, "Numerical study of the stress-strain state of one- and three-layer plates and shells of complex geometry," *Sov. Appl. Mech.*, **19**, No. 7, 583–588 (1983).
18. A. R. Shahidi et al., "Nonlinear static analysis of arbitrary quadrilateral plates in very large deflections," *Communic. Nonlin. Sci. Numer. Simul.*, **12**, 832–848 (2007).
19. I. Shufrin et al., "A semi-analytical approach for the geometrically nonlinear analysis of trapezoidal plates," *Int. J. Mech. Sci.*, **52**, 1588–1596 (2010).
20. R. S. Srinivasan and S. V. Ramachandran, "Large deflection of clamped skew plates," *Comp. Meth. Appl. Mech. Eng.*, **7**, 219–233 (1976).